Received: 6 December 2021 | Revised: 4 February 2022 | Accepted: 28 February 2022 | Published on: 4 April 2022

DOI: 10.1002/mrm.29240

TECHNICAL NOTE

Magnetic Resonance in Medicine

Optimal saturation recovery time for minimizing the underestimation of arterial input function in quantitative cardiac perfusion MRI

Lexiaozi Fan[1,2] | **Kyungpyo Hong**[1] | **Li-Yueh Hsu**[3] | **James C. Carr**[1] | **Bradley D. Allen**[1] | **Daniel C. Lee**[4] | **Daniel Kim**[1,2]

[1]Department of Radiology, Northwestern University Feinberg School of Medicine, Chicago, Illinois, USA

[2]Department of Biomedical Engineering, Northwestern University, Evanston, Illinois, USA

[3]Department of Radiology and Imaging Sciences, National Institutes of Health, Bethesda, Maryland, USA

[4]Division of Cardiology, Internal Medicine, Northwestern University Feinberg School of Medicine, Chicago, Illinois, USA

Correspondence
Lexiaozi Fan, Department of Radiology, Northwestern University, 737 N. Michigan Avenue, Suite 1600, Chicago, IL 60611, United States.
Email: lexiaozifan2019@u.northwestern.edu

Funding information
American Heart Association, Grant/Award Number: 19IPLOI34760317; National Institutes of Health, Grant/Award Numbers: R01HL116895, R01HL138578, R01HL151079, R21AG055954, R21EB024315, R21EB030806A1

Purpose: The purpose of this study was to determine an optimal saturation-recovery time (TS) for minimizing the underestimation of arterial input function (AIF) in quantitative cardiac perfusion MRI without multiple gadolinium injections per subject.

Methods: We scanned 18 subjects (mean age = 59 ± 14 years, 9/9 males/females) to acquire resting perfusion data and 1 additional subject (age = 38 years, male) to obtain stress-rest perfusion data using a 5-fold accelerated pulse sequence with radial k-space sampling and applied k-space weighted image contrast (KWIC) filters on the same k-space data to retrospectively reconstruct five AIF images with effective TS ranging from 10 to 21.2 ms (2.8 ms steps). Undersampled images were reconstructed using a compressed sensing framework with temporal-total-variation and temporal-principal-component as 2 orthogonal sparsifying transforms. The image processing steps included, same motion correction across five different AIF images, signal normalization by the proton-density-weighted-image, signal-to-T_1 conversion using a Bloch equation, T_1-to-gadolinium-concentration conversion assuming fast water exchange, T_2* correction to the AIF, and gadolinium-concentration to myocardial blood flow (MBF) conversion based on a Fermi model.

Results: Among five TS values, the shortest TS (10 ms) produced significantly ($P < 0.05$) higher peak AIF and lower resting MBF (13.73 mM, 0.73 mL g^{-1} min^{-1}) than 12.8 ms (11.24 mM, 0.89 mL g^{-1} min^{-1}), 15.6 ms (9.56 mM, 1.05 mL g^{-1} min^{-1}), 18.4 ms (8.55 mM, 1.17 mL g^{-1} min^{-1}), and 21.2 ms (7.95 mM, 1.27 mL g^{-1} min^{-1}). Similarly, shorter TS reduced underestimation of AIF (or overestimation of MBF) for both during stress and at rest, but this effect was canceled in myocardial-perfusion-reserve (MPR).

Conclusion: This study demonstrates that TS of 10 ms reduces the underestimation of AIF and, hence, the overestimation of MBF compared with longer TS values (12.8-21.2 ms).

KEYWORDS

arterial input function, k-space weighted image contrast filters, myocardial blood flow, radial k-space, saturation recovery time

1 | INTRODUCTION

Coronary artery disease (CAD) is a leading cause of sickness and death in the United States.[1] Noninvasive myocardial perfusion imaging modalities such as single-photon emission computerized tomography (SPECT), (positron emission tomography) PET, and cardiovascular magnetic resonance (CMR) play an important role as a gatekeeper to cardiac catheterization.[2] CMR offers several advantages over SPECT and PET, including high spatial resolution, lack of ionizing radiation, and capability to provide additional information such as myocardial function, edema, and scarring/fibrosis and hemodynamics evaluation with a single examination. Although a qualitative evaluation of perfusion CMR is the clinical norm, myocardial blood flow (MBF) quantification from perfusion CMR images offers incremental value, including: improved diagnostic accuracy,[3] particularly in multi-vessel obstructive disease and microvascular dysfunction[4]; prognostic value[5,6]; and improved precision for longitudinal studies.

There are several technical challenges to achieve high accuracy in MBF quantification, including, but not limited to, low signal-to-noise ratio (SNR), nonlinear relationship between the measured signal and concentration of gadolinium ([Gd]), and T_2* decay in arterial input function (AIF) signal at peak blood enhancement because of high [Gd] during first-passage. This study revisits the accuracy in AIF, which is often underestimated because of high [Gd] (>5 mM) in the left ventricular (LV) blood pool at peak enhancement. The two main imaging approaches to compensate for this nonlinearity issue are the dual-bolus[7] and dual-imaging methods.[8,9] The dual-bolus technique, wherein the AIF image is acquired with a low [Gd] and tissue function (TF) images are acquired with a high [Gd], is not practical in a busy radiology clinic because it requires contrast dilution and twice as many bolus injections and image acquisitions. Furthermore, a meticulous setup is necessary to assure that 2 different concentrations are at equal volumes and prevent backflow of solutions in the injector apparatus between saline and gadolinium syringes.[10] A more practical approach is to perform one set of stress-rest imaging with the dual-imaging sequence,[8,9,11,12] wherein the AIF images are acquired with a short saturation recovery time (TS) to sample the center of k-space and TF images are acquired with a long TS.

The previous studies utilizing the dual-imaging method[8,9,11,12] used TS ranging from 20-27 ms to linearize the relationship between the AIF signal and [Gd], in order to reduce the underestimation of AIF. However, none of the studies have investigated an optimal TS for minimizing the underestimation of AIF. The main reason why it is impractical to conduct such a study is that it requires multiple injections of gadolinium. In this study, we sought to identify an optimal TS for minimizing the underestimation of AIF without multiple injections of gadolinium per subject. This was accomplished by scanning patients using a radial k-space sampling pattern with a minimum TS of 10 ms and retrospectively reconstructing five different AIF images derived from the same radial k-space data with effective TS ranging from 10 to 21.2 ms (2.8 ms steps) using k-space weighted image contrast (KWIC) filters.[13]

2 | METHODS

2.1 | Study population

All patients provided consent in writing. This study was performed in accordance with protocols approved by our institutional review board and was Health Insurance Portability and Accountability Act (HIPAA) compliant. We prospectively enrolled 18 patients (mean age = 59 ± 14 years, 9/9 males/female) with left ventricular ejection fraction (LVEF) > 50% and no evidence of vascular late gadolinium enhancement to acquire resting perfusion data: 13 patients were enrolled in a study examining the chronic (medium days since hospitalization = 102 days) impact of coronavirus disease (COVID-19) on the heart; 3 patients were enrolled in a study examining heart failure (HF) with recovered LVEF; 2 subjects were volunteers. In addition, 1 patient (age = 38 years, male) with pulmonary hypertension, dilated right ventricle, and right ventricular dysfunction was enrolled to acquire stress-rest perfusion data, and another subject (age = 46 years, male) was scanned to collect resting perfusion data to determine the lower limit of TS that achieves a good balance between linearity and SNR. Our justification for mixing data from different patient cohorts is based on our stated goal to identify an optimal TS for minimizing the underestimation of AIF. Other clinical profiles were omitted because they were irrelevant to this technical study.

2.2 | MRI hardware

MRI was performed on one 1.5 T whole-body MRI scanner (MAGNETOM Aera, Siemens Healthineers, Erlangen, Germany) equipped with a gradient system capable of achieving a maximum gradient strength of 45 mT m^{-1} and a slew rate of 200 T m^{-1} s^{-1}. MRI signal reception was made using anterior and posterior coil arrays with 30 total coil elements.

2.3 | Pulse sequence

Relevant imaging parameters for our 2D multi-slice cardiac perfusion pulse sequence using gradient

echo readout with radial k-space sampling included: FOV = 384 mm × 384 mm, matrix size =192 × 192, spatial resolution = 2 mm × 2 mm, slice thickness = 8 mm, TE/TR = 1.5/2.8 ms, flip angle = 15°, minimum TS = 10 ms, B_1-insensitive hybrid pulse train as the saturation pulse,[14] 38 radial spokes per frame (corresponding to an acceleration factor of 5), single-shot readout duration per frame = 106 ms, 100 repetitions, electrocardiogram triggering every heartbeat, and 4-7 slices per heartbeat depending on heart rate. Each patient was instructed to breathe normally during scanning. For more details on the pulse sequence, please see Naresh et al.[12] Each perfusion scan was performed with administration of either 0.075 (estimated glomerular filtration rate [eGFR] = 45-60) or 0.1 mmol kg^{-1} (eGFR > 60) of gadobutrol (Gadavist, Bayer HealthCare, Whippany, USA) at 3 mL s^{-1} via a power injector.

2.4 | Minimum TS determination

We elected minimum TS as 10 ms to achieve a good balance between linearity and SNR. To support our choice, we conducted a theoretical analysis and scanned a T_1mes phantom and one additional subject at rest to identify the lower bound of TS that achieves a good balance between linearity and SNR. For details, please see *Minimum TS experiment* in Supporting Information.

2.5 | Monte Carlo simulation: SNR for TF images

Intrinsic SNR is a critical ingredient for achieving high accuracy in MBF quantification. We performed a theoretical analysis to estimate the intrinsic SNR of TF images, to justify KWIC filtering to achieve TS of 113.6 ms for TF images. For additional details, please see *Monte Carlo analysis* in Supporting Information.

2.6 | KWIC filters

In radial k-space sampling, the center of k-space is sampled by each radial spoke. This provides an opportunity to retrospectively choose an arbitrary TS by applying KWIC filters. For myocardial wall assessment, images were reconstructed using a KWIC filter to exclude the first 19 radial spokes and maintain the center of the last radial spoke only (i.e., effective TS = 113.6 ms as shown in Figure 1) to maximize the SNR (see the *Monte Carlo analysis* in Supporting Information). To determine an optimal TS for minimizing the underestimation of AIF, five different KWIC filtered images were reconstructed from the same raw k-space data by maintaining the center of k-space from the first to fifth radial spoke only (i.e., effective TS from 10-21.2 ms [2.8 ms steps] as shown in Figure 1). Because the expected AIF signal is relatively low for the first to fifth radial spokes, we zeroed out the outer one third of k-space in the frequency-encoding direction, to reduce noise and aliasing artifacts.

2.7 | Image reconstruction

We applied KWIC filters as a pre-processing step before compressed sensing[15] reconstruction of AIF and TF images from the same raw k-space data. To accelerate image reconstruction, coil compression was used to produce 8 virtual coils,[16] and gpuNUFFT[17] was used throughout the reconstruction pipeline. The multi-coil k-space datasets were reconstructed using compressed sensing with temporal total variation and temporal PCA (TPCA) as the 2 orthogonal sparsifying transforms and nonlinear conjugate gradient with backtracking line search as the optimization algorithm with 30 iterations. Normalized regularization weight for temporal total variation was set as 0.005 (0.003 for TF images) of the maximum signal of the reconstructed image in each iteration, and normalized regularization weight for TPCA was set as one quarter of temporal total variation. We established the optimal regularization weights by sweeping over a range from 0.001 to 0.01 (0.001 steps) to identify an optimal regularization weight that achieves a good balance between suppression of aliasing artifacts and temporal blurring of myocardial wall motion. We determined this optimal regularization weight based on visual inspection of 6 training datasets. For more details on the image reconstruction pipeline, please see reference.[12]

2.8 | MBF quantification

Image processing was conducted by one investigator (L.F.). Five pixel-by-pixel MBF maps (same TF image, five different AIF images) were quantified for each slice using the following steps as shown in Figure 2. First, the motion correction was conducted on the TF images using a previously described method.[18] The same deformation field from the TF image was then applied to all 5 AIF images to ensure consistency. Second, T_1-weighted images were normalized by the corresponding PD-weighted images to correct for the unknown equilibrium of magnetization and the surface-coil effects.[19] Third, the normalized signal was converted to [Gd] using the Bloch equation described by Mendes et al.,[20] using 5.3 and 5.2 mM^{-1} s^{-1}

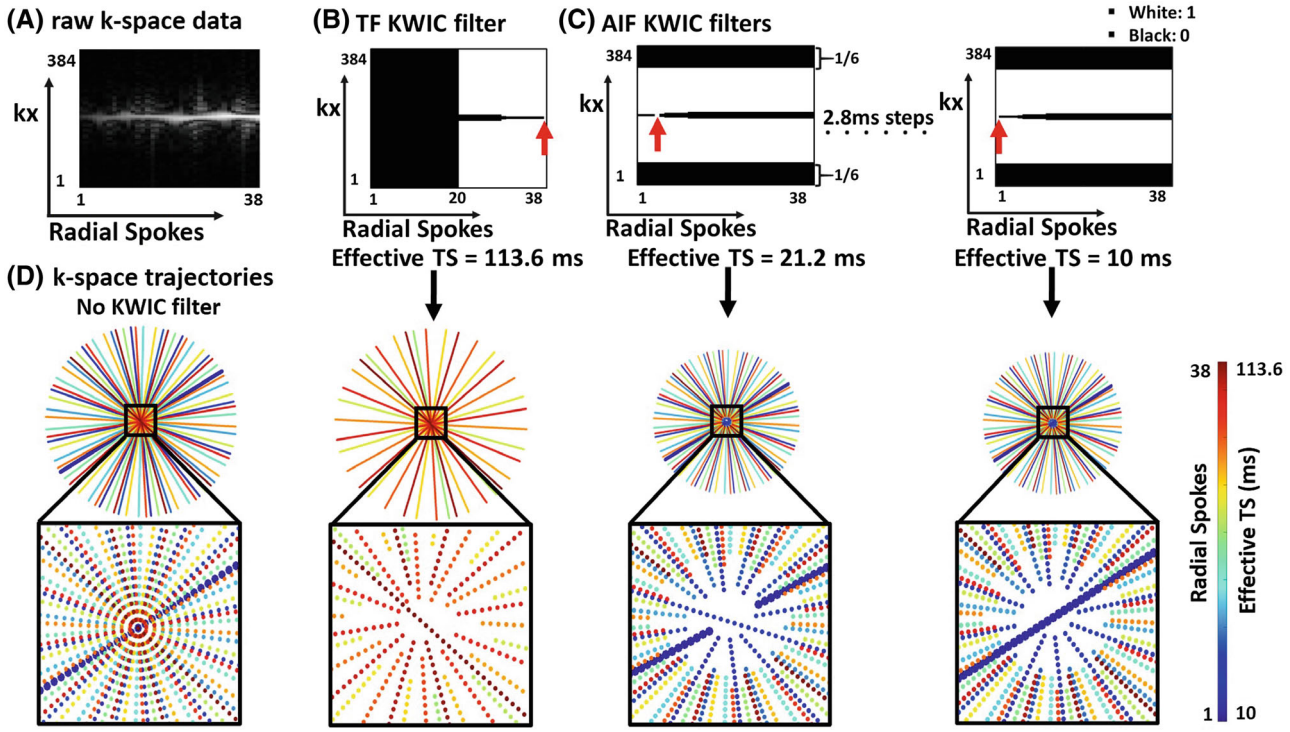

FIGURE 1 (A) Raw k-space data; KWIC filters used for TF (B) and AIF (C) image reconstruction. For TF, the effective TS after the particular KWIC was 113.6 (= 10 + 2.8 × 37) ms. For AIF, five different KWIC filters were applied to generate five different images with effective TS ranging from 10 to 21.2 ms (2.8 ms steps). (D) k-Space trajectories without and with KWIC filters. The darkest blue line represents the first radial spoke. The color bar indicates the radial spoke number following the saturation pulse (i.e., k-space ordering) or effective TS. KWIC, k-space-weighted image contrast; TF, tissue function; AIF, arterial-input-function; TS, saturation-recovery time

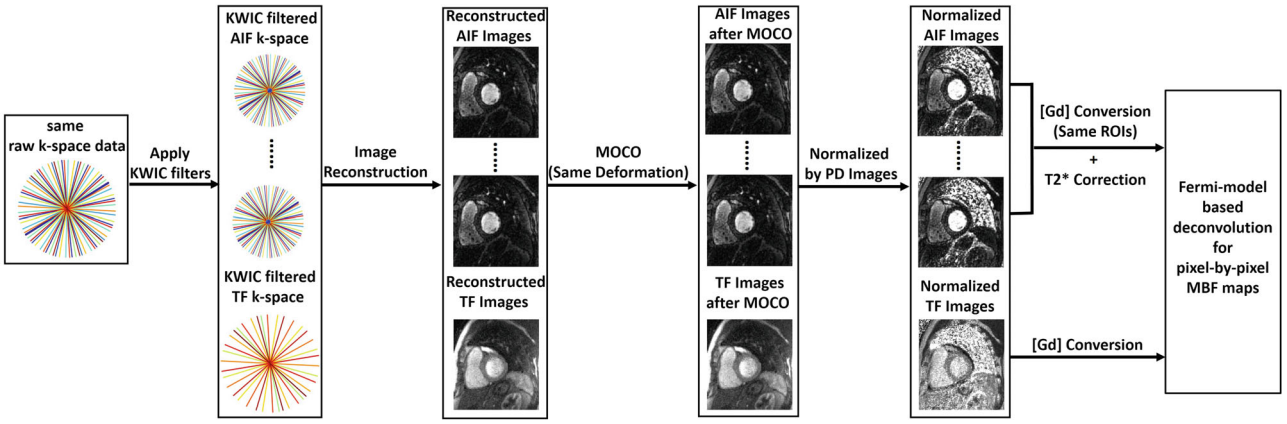

FIGURE 2 A schematic overview of the image reconstruction and processing pipeline for radial perfusion data obtained during free breathing. The sequence of steps includes: KWIC filtering of the radial k-space data, compressed sensing reconstruction of undersampled and filtered images, motion correction, signal normalization, [Gd] calculation (T_2* correction to the AIF), Fermi-model deconvolution for pixel-by-pixel MBF quantification. MOCO, motion correction; KWIC, k-space-weighted image contrast; [Gd], gadolinium concentration; AIF, arterial-input-function; MBF, myocardial blood flow

as γ_1 of gadobutrol in the blood and myocardium, respectively,[21] and assuming fast water exchange.[22] The AIF signal-time curves were derived by manually drawing a region of interest inside the left ventricular cavity. For consistency, the same region of interest was used for all five reconstructed AIF images. Fourth, T_2* decay in the AIF was corrected using the previously described theoretical approach.[23] Fifth, pixel-wise MBF maps were quantified using a Fermi function[24] as the transfer function to deconvolve the myocardial perfusion [Gd]-time curves with the

AIF. To speed up data processing, we cropped the field of view to exclude extra cardiac tissues. For more details on the quantification of MBF, please see Naresh et al.[12]

2.9 | Statistical analysis

The statistical analyses were conducted by one investigator (L.F.). A Lilliefors test was performed to test the null hypothesis that both peak AIF and mean resting MBF is normally distributed at the 5% significance level. We compared both the peak AIF and mean resting MBF values calculated from the AIF images reconstructed with five different effective TS using repeated measures ANOVA with Bonferroni correction as the post hoc test for rest perfusion data. A $P < 0.05$ was considered statistically significant.

3 | RESULTS

According to the Lilliefors test, both the peak AIF and resting MBF were normally distributed (statistic: [0.05, 0.2]; $P > 0.05$) for the five different effective TS groups.

Figure 3A shows theoretical plots of the normalized signal as a function of ground truth [Gd] for five different TS values (10 ms, 12.8 ms, 15.6 ms, 18.4 ms, and 21.2 ms). As shown, shorter TS achieves a higher degree of linearization between the normalized signal and [Gd] at the expense of lower normalized signal (i.e., SNR). Figure 3B shows actual plots of the AIF signal-time curves and the corresponding AIF [Gd]-time curves without and with T_2* correction from one representative patient. Although shorter TS produced lower signal (i.e., SNR), it resulted in higher AIF because of better linearity compared with longer TS values. T_2* correction does not impact the overall comparison across TS. Figure 3C shows the corresponding resting MBF maps; MBF increased with effective TS because of underestimation of AIF.

Four subjects were excluded from AIF and resting MBF quantifications because of poor image quality or motion correction. As summarized in Table 1 ($n = 14$), compared to TS = 10 ms, higher TS resulted in significantly decreased peak AIF as well as significantly increased MBF (both $P < 0.05$). Specifically, the peak AIF was 13.73 ± 2.25, 11.24 ± 1.77, 9.56 ± 1.45, 8.55 ± 1.32, and 7.95 ± 1.24 mM for TS 10, 12.8, 15.6, 18.4, and 21.2 ms, respectively; the corresponding resting MBF was 0.73 ± 0.12, 0.89 ± 0.15, 1.05 ± 0.17, 1.17 ± 0.19, and 1.27 ± 0.21 mL g^{-1} min^{-1} for TS 10, 12.8, 15.6, 18.4, and 21.2 ms, respectively.

Figure 4A shows actual plots of the AIF [Gd]-time curves with T_2* correction and the corresponding MBF maps during stress for different TS values; Figure 4B shows the corresponding data at rest; Figure 4C shows the myocardial perfusion reserve (MPR) values. Consistent with the remaining resting perfusion data, shorter TS reduced underestimation of AIF (or overestimation of

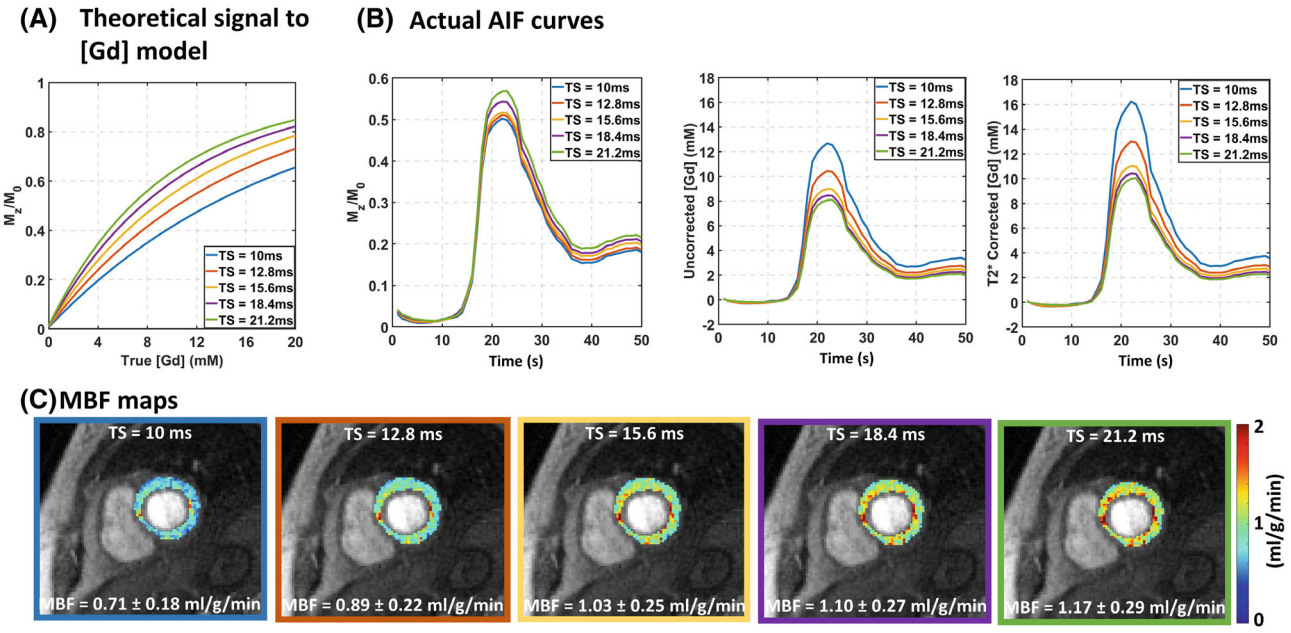

FIGURE 3 (A) Theoretical plots describing nonlinear relationships between the normalized signal and [Gd] for five different TS values. (B) Example plots of the AIF signal-time curves and AIF [Gd]-time curves without and with T_2* correction from one representative patient. (C) The corresponding resting MBF maps from five different AIFs with mean and SD values as shown. [Gd], gadolinium concentration; TS, saturation-recovery time; AIF, arterial-input-function; MBF, myocardial blood flow

TABLE 1 A statistical summary of peak AIF and resting MBF values from 14 subjects

TS	10 ms	12.8 ms	15.6 ms	18.4 ms	21.2 ms
AIF (mM)	13.73 ± 2.25	11.24 ± 1.77*	9.56 ± 1.45*	8.55 ± 1.32*	7.95 ± 1.24*
MBF (mL g^{-1} min^{-1})	0.73 ± 0.12	0.89 ± 0.15*	1.05 ± 0.17*	1.17 ± 0.19*	1.27 ± 0.21*

Note: Reported values represent mean ± SD. Compared with TS = 10 ms as the control, both AIF and MBF values for different TS values were significantly different.
*$P < 0.05$.

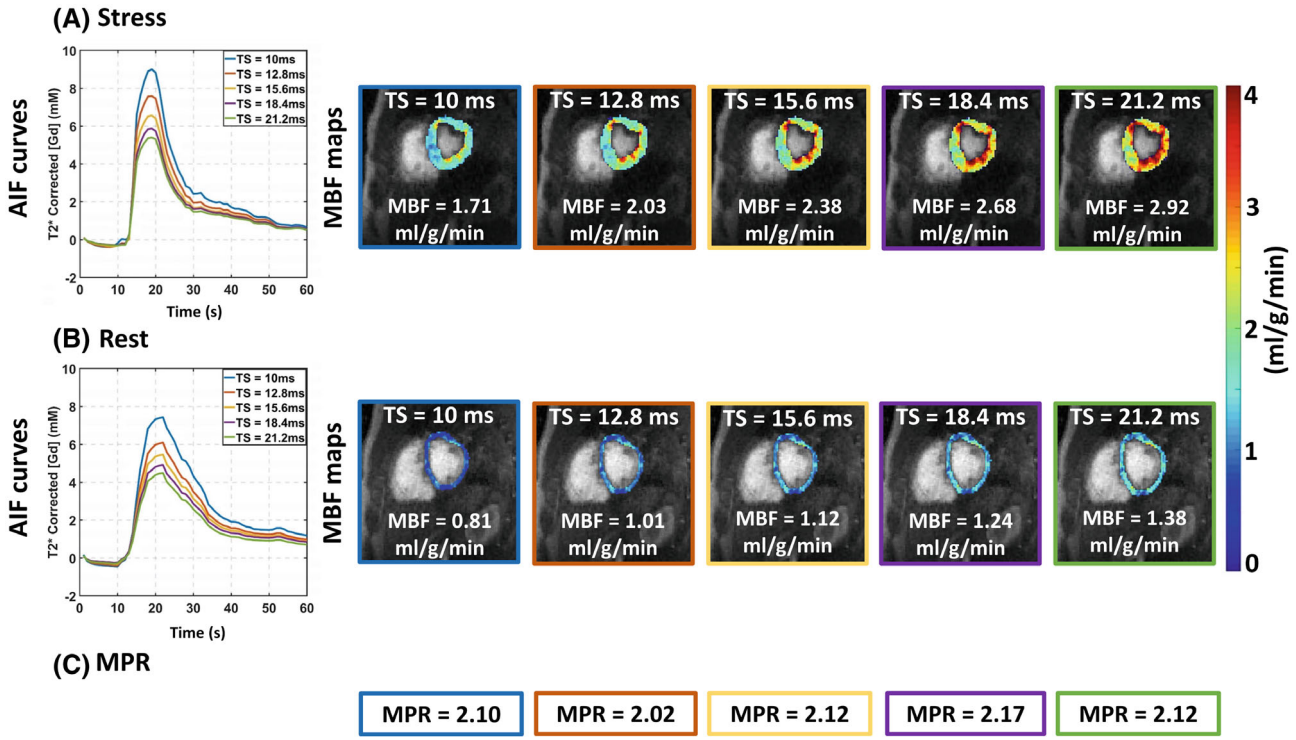

FIGURE 4 (A) Actual plots of the AIF [Gd]-time curves with T_2* correction and the corresponding MBF maps during stress for different TS values; (B) the corresponding data at rest; (C) the MPR values. AIF, arterial-input-function; [Gd], gadolinium concentration; MBF, myocardial blood flow; TS, saturation-recovery time; MPR, myocardial perfusion reserve

MBF) for both stress and rest data. However, MPR did not change significantly with TS, because the impact of underestimation of AIF on MBF is canceled in MPR.

4 | DISCUSSION

This study highlights the importance of reducing TS as short as 10 ms for reducing the underestimation of AIF and the overestimation of MBF. Although previous dual-imaging studies[8,9,11,12] used a short TS ranging from 20-27 ms, this work represents the first study comparing multiple TS values (10-21.2 ms) to determine an optimal TS (10 ms) for further minimizing the underestimation of AIF.

This study has several interesting points. First, we acquired resting perfusion data using radial k-space sampling with a minimum TS of 10 ms and retrospectively reconstructing five different AIF images derived from the same radial k-space data with TS ranging from 10 to 21.2 ms (2.8 ms steps) using KWIC filters. This experimental design enabled us to identify an optimal TS for AIF without the complexity of multiple injections of gadolinium as well as image acquisitions. Second, to reduce variables, we applied the same deformation fields to all five AIF images to correct for respiratory motion, the same region of interest to obtain the AIF signal-time curves, and the same TF image with matching cardiac contours. We found the peak AIF and resting MBF values were significantly different between the five TS values. Given the lack of ground truth for AIF and MBF, we infer literature values. The resting MBF (0.73 mL g^{-1} min^{-1}) calculated from AIF with TS of 10 ms agrees better with the resting MBF reported by two cardiac PET studies[25]: (1) mean resting MBF = 0.71 mL g^{-1} min^{-1} in 363 healthy subjects using ^{13}N-ammonia and (2) mean

resting MBF = 0.74 mL g^{-1} min^{-1} in 382 healthy subjects using ^{82}Rb. We note that this comparison across different cohorts and modalities should be interpreted with caution, because there are numerous unaccounted variables. Third, compared with TS of 21.2 ms, which is similar to TS of 23.8 ms proposed by the widely used quantitative cardiac perfusion sequence,[11] TS of 10 ms increased AIF by 73% and decreased resting MBF by 43%. Our finding suggests the pulse sequence proposed by Kellman et al[11] may overestimate MBF because of the underestimation of AIF. This problem is fixable by redesigning the pulse sequence to use TS of 10 ms for AIF scanning. Fourth, our finding suggests that the impact of the underestimation of AIF may be negligible for calculation of MPR, because the underestimation/overestimation effect on AIF/MBF is canceled in MPR. However, more data from greater number of patients are needed to validate our initial finding.

This study has several limitations that warrant further discussion. First, this study applied KWIC filtering to retrospectively select an effective TS. KWIC filters zero out the central parts of k-space, but they retain signal from other parts of k-space. Our signal model does not account for these residual signals, which may result in a bias in [Gd] calculation. The potential bias should be consistent across the five TS values because we applied similarly shaped KWIC filters, suggesting that the observed trend across TS should be valid. An alternative approach is to perform multiple TS acquisitions using a Cartesian k-space sampling pulse sequence. However, such an approach is impractical because it necessitates multiple injections of gadolinium, requires compensation of residual gadolinium from previous injections, compensates for variations in physiology (e.g., heart rate, breathing pattern) and manual data analysis (segmentation), and increased safety concerns associated with gadolinium. Second, this study did not evaluate whether the observed trend is maintained at 3 T. Although there is no theoretical basis to expect a different trend, a future 3 T study is warranted for verification. Third, this study lacks ground truths for AIF and MBF to truly validate our approach. This is a common problem for all quantitative cardiac first-pass perfusion studies in patients, unless one is able to conduct a PET-MR study on the same day, which has its own challenges (limited available of equipment and radiotracer). Given these challenges, we elected to compare our results to 2 previous PET studies. Fourth, this study only included 1 patient scan during stress testing. More data from a greater number of patients during stress testing are needed to validate our findings.

In summary, we conclude that an AIF scan with TS of 10 ms minimizes the underestimation of AIF and, hence, minimizes the overestimation of MBF compared with TS from 20 to 27 ms.

ACKNOWLEDGMENTS

We thank funding support from the National Institutes of Health (R01HL116895, R01HL138578, R21EB024315, R21AG055954, R01HL151079, and R21EB030806A1) and American Heart Association (19IPLOI34760317). We also thank Dr. Benjamin Freed for allowing us to scan 1 of his patients during stress and at rest. We also thank Center for Translational Imaging Cardiovascular Imaging for use of its facility to conduct phantom experiments.

CONFLICT OF INTEREST

None of the authors have relationships with industry related to this study.

DATA AVAILABILITY STATEMENT

The data that support the findings of this study are available from the corresponding author (L.F.) on reasonable request.

ORCID

Lexiaozi Fan https://orcid.org/0000-0002-3714-5372
Kyungpyo Hong https://orcid.org/0000-0002-9453-6580
Daniel Kim https://orcid.org/0000-0003-2660-8973

REFERENCES

1. Benjamin EJ, Muntner P, Alonso A, et al. Heart Disease and Stroke Statistics-2019 update: a report from the American Heart Association. *Circulation*. 2019;139:e56-e528.
2. Patel MR, Peterson ED, Dai D, et al. Low diagnostic yield of elective coronary angiography. *N Engl J Med*. 2010;362:886-895.
3. Mordini FE, Haddad T, Hsu LY, et al. Diagnostic accuracy of stress perfusion CMR in comparison with quantitative coronary angiography: fully quantitative, semiquantitative, and qualitative assessment. *JACC Cardiovasc Imaging*. 2014;7:14-22.
4. Patel AR, Antkowiak PF, Nandalur KR, et al. Assessment of advanced coronary artery disease: advantages of quantitative cardiac magnetic resonance perfusion analysis. *J Am Coll Cardiol*. 2010;56:561-569.
5. Brown LAE, Onciul SC, Broadbent DA, et al. Fully automated, inline quantification of myocardial blood flow with cardiovascular magnetic resonance: repeatability of measurements in healthy subjects. *J Cardiovasc Magn Reson*. 2018;20:48.
6. Knott KD, Seraphim A, Augusto JB, et al. The prognostic significance of quantitative myocardial perfusion: an artificial intelligence-based approach using perfusion mapping. *Circulation*. 2020;141:1282-1291.
7. Christian TF, Rettmann DW, Aletras AH, et al. Absolute myocardial perfusion in canines measured by using dual-bolus first-pass MR imaging. *Radiology*. 2004;232:677-684.
8. Gatehouse PD, Elkington AG, Ablitt NA, Yang GZ, Pennell DJ, Firmin DN. Accurate assessment of the arterial input function during high-dose myocardial perfusion cardiovascular magnetic resonance. *J Magn Reson Imaging*. 2004;20:39-45.
9. Kim D, Axel L. Multislice, dual-imaging sequence for increasing the dynamic range of the contrast-enhanced blood signal and

CNR of myocardial enhancement at 3T. *J Magn Reson Imaging*. 2006;23:81-86.
10. Chatterjee N, Benefield BC, Harris KR, Fluckiger JU, Carroll T, Lee DC. An empirical method for reducing variability and complexity of myocardial perfusion quantification by dual bolus cardiac MRI. *Magn Reson Med*. 2017;77:2347-2355.
11. Kellman P, Hansen MS, Nielles-Vallespin S, et al. Myocardial perfusion cardiovascular magnetic resonance: optimized dual sequence and reconstruction for quantification. *J Cardiovasc Magn Reson*. 2017;19:43.
12. Naresh NK, Haji-Valizadeh H, Aouad PJ, et al. Accelerated, first-pass cardiac perfusion pulse sequence with radial k-space sampling, compressed sensing, and k-space weighted image contrast reconstruction tailored for visual analysis and quantification of myocardial blood flow. *Magn Reson Med*. 2019;81:2632-2643.
13. Song HK, Dougherty L. K-space weighted image contrast (KWIC) for contrast manipulation in projection reconstruction MRI. *Magn Reson Med*. 2000;44:825-832.
14. Kim D, Oesingmann N, McGorty K. Hybrid adiabatic-rectangular pulse train for effective saturation of magnetization within the whole heart at 3 T. *Magn Reson Med*. 2009;62:1368-1378.
15. Lustig M, Donoho D, Pauly JM. Sparse MRI: the application of compressed sensing for rapid MR imaging. *Magn Reson Med*. 2007;58:1182-1195.
16. Huang F, Vijayakumar S, Li Y, Hertel S, Duensing GR. A software channel compression technique for faster reconstruction with many channels. *Magn Reson Imaging*. 2008;26:133-141.
17. Knoll F, Schwarzl A, Diwoky C & Sodickson DK gpuNUFFT-an open source GPU library for 3D regridding with direct Matlab interface. In: Proceedings of the 22rd Annual Meeting of ISMRM, Melbourne, Australia 2014. Abstract No. 4297.
18. Benovoy M, Jacobs M, Cheriet F, Dahdah N, Arai AE, Hsu LY. Robust universal nonrigid motion correction framework for first-pass cardiac MR perfusion imaging. *J Magn Reson Imaging*. 2017;46:1060-1072.
19. Cernicanu A, Axel L. Theory-based signal calibration with single-point T1 measurements for first-pass quantitative perfusion MRI studies. *Acad Radiol*. 2006;13:686-693.
20. Mendes JK, Adluru G, Likhite D, et al. Quantitative 3D myocardial perfusion with an efficient arterial input function. *Magn Reson Med*. 2020;83:1949-1963.
21. Rohrer M, Bauer H, Mintorovitch J, Requardt M, Weinmann HJ. Comparison of magnetic properties of MRI contrast media solutions at different magnetic field strengths. *Invest Radiol*. 2005;40:715-724.
22. Donahue KM, Weisskoff RM, Burstein D. Water diffusion and exchange as they influence contrast enhancement. *J Magn Reson Imaging: JMRI*. 1997;7:102-110.
23. Fan L, Allen BD, Culver AE, et al. A theoretical framework for retrospective T 2 * correction to the arterial input function in quantitative myocardial perfusion MRI. *Magn Reson Med*. 2021;86:1137-1144.
24. Jerosch-Herold M, Wilke N, Stillman AE. Magnetic resonance quantification of the myocardial perfusion reserve with a Fermi function model for constrained deconvolution. *Med Phys*. 1998;25:73-84.
25. Murthy VL, Bateman TM, Beanlands RS, et al. Clinical quantification of myocardial blood flow using PET: joint position paper of the SNMMI cardiovascular council and the ASNC. *J Nucl Med*. 2018;59:273-293.

SUPPORTING INFORMATION

Additional supporting information may be found in the online version of the article at the publisher's website.

Figure S1 (A) T_1 maps of T_1mes phantom calculated acquired using three different TS values; (B) the corresponding difference maps, where TS = 278 ms is the reference.

Figure S2 (A) Five different KWIC filtered CS reconstructed images by maintaining the center from the first to the fifth radial spoke only (i.e., effective TS from 5 to 16.2 ms [2.8 ms steps]); (B) corresponding PD normalized images; (C) theoretical plots describing the nonlinear relationships between the normalized signal and [Gd] for five different TS values; (D) plots of the AIF signal-time curves from one patient acquired with minimal TS = 5 ms.

How to cite this article: Fan L, Hong K, Hsu L-Y, et al. Optimal saturation recovery time for minimizing the underestimation of arterial input function in quantitative cardiac perfusion MRI. *Magn Reson Med*. 2022;88:832-839. doi: 10.1002/mrm.29240